

Anomalous alignment dependence of the third-order harmonic of H_2^+ ions in intense laser fieldsYing-Jun Jin,¹ Xiao-Min Tong,^{1,2,*} and Nobuyuki Toshima¹¹*Division of Materials Science, Faculty of Pure and Applied Sciences, University of Tsukuba, 1-1-1 Tennodai, Tsukuba, Ibaraki 305-8577, Japan*²*Center for Computational Sciences, University of Tsukuba, 1-1-1 Tennodai, Tsukuba, Ibaraki 305-8577, Japan*

(Received 16 October 2012; published 26 November 2012)

We studied the high-harmonic generation of H_2^+ ions in an intense laser field by solving the time-dependent Schrödinger equation in prolate spheroidal coordinates. By analyzing the power spectra of the harmonics with the electric field polarized along the molecular axis, we found that the yield of the third-order harmonic drops by several orders of magnitude at a specified aligned angle between the laser polarization direction and the molecular axis. The laser polarization angle of the minimum depends on the internuclear distance and it disappears both in the separated- and united-atom limits. This infers that the minimum is associated with the molecular symmetry. By decomposing individual contributions of the σ and π states, we identified that the minimum is attributed to the cancellation of the induced dipole moments of the σ and π states, like a dynamical Cooper minimum, but the position of the minimum can be tuned by the laser intensity for a given internuclear distance.

DOI: [10.1103/PhysRevA.86.053418](https://doi.org/10.1103/PhysRevA.86.053418)

PACS number(s): 33.80.Rv, 42.65.Ky, 33.20.Xx

I. INTRODUCTION

High-harmonic generation (HHG) has been a popular research topic since it was discovered in late 1980s [1,2]. The mechanism of the HHG was explained by the three-step model proposed by Corkum [3]. Since then, extensive studies have been done on how to generate a very-high-energy HHG [4–7] and how to generate an intense HHG through phase-matched generation [8–10] or a dual-gas multijet array [11–13]. The created attosecond pulse [14–16] or pulse train [17,18] can be used as a coherent XUV source to study dynamics in femtosecond [19–21] or even attosecond time domains [22,23]. Although the mechanism of the HHG is known, the HHG of atoms and molecules in an intense laser field has to be studied case by case, since the HHG is a nonlinear process depending on the details of the atomic and molecular structures. For example, the HHG yields can be enhanced significantly at certain nuclear separations for H_2^+ molecular ions [24], and the yields can be tuned by the alignment of the molecular ions to the laser polarization [25].

The HHG can also be used to extract information regarding the electronic structure of molecules [26–28], and a recent experiment has revealed the Cooper minimum [29] of N_2 by molecular frame high-harmonic spectroscopy [30]. Stimulated by these developments, we investigate the HHG of H_2^+ in an intense laser field. We found that the yield of the third-order harmonic with its electric field polarized along the molecular axis has a minimum when the laser field is along a certain angle with respect to the molecular axis. The position of this Cooper-like minimum [29] can be tuned by the laser intensity. The angle of the minimum also depends on the internuclear distance. By decomposing contributions from the molecular wave functions with different symmetries, we show that the minimum is associated with the cancellation of the induced dipole moments from the σ states and π states. Although the account of the induced dipole component perpendicular to the molecular axis may wash out the minimum, such a

minimum could still be observed by the molecular frame high-harmonic spectroscopy [30]. The minimum can be used to obtain information regarding the internuclear distance, the laser property, and the molecular alignment parameters in the molecular ion beam experiments [31].

II. THEORETICAL METHOD

We calculate the HHG by solving the time-dependent Schrödinger equation in prolate spheroidal coordinates, which are suitable for describing two-center problems properly. Here we brief only on the central equations, and the details of the numerical procedure can be found in our previous papers [32,33]. The time-dependent electron wave function $\Psi(t)$ of H_2^+ at a fixed internuclear distance satisfies the following equation (atomic units $\hbar = m = e = 1$ are used unless stated otherwise):

$$i \frac{\partial}{\partial t} \Psi(t) = [H_0 + V_{\text{ext}}(t)] \Psi(t). \quad (1)$$

H_0 , the laser-field free Hamiltonian of H_2^+ , is read as

$$H_0 = -\frac{1}{2} \nabla^2 - \frac{1}{r_1} - \frac{1}{r_2} + \frac{1}{2a}, \quad (2)$$

where r_1 (r_2) is the distance between the electron and nucleus one (two). The electron laser interaction $V_{\text{ext}}(t)$ is written as

$$V_{\text{ext}}(t) = F(t)[a\xi\eta \cos\theta + a\sqrt{(\xi^2 - 1)(1 - \eta^2)} \cos\varphi \sin\theta], \quad (3)$$

where $a = R/2$, with R the internuclear distance, and θ the angle of the laser polarization with respect to the molecular axis. $F(t)$, the linearly polarized time-dependent laser field strength, is written as

$$F(t) = E_0 e^{-2 \ln 2 t^2 / \tau^2} \cos(\omega t), \quad (4)$$

with E_0 the peak field strength, τ the full width at half maximum of the pulse duration, and ω the center frequency of the intense laser. Here we assume that the laser polarization is in the xz plane. ξ , η , and φ are the prolate spheroidal

*tong.xiaomin.ga@u.tsukuba.ac.jp

coordinates, which are related to Cartesian coordinates x , y , and z as

$$x = a\sqrt{(\xi^2 - 1)(1 - \eta^2)} \cos \varphi, \quad (5)$$

$$y = a\sqrt{(\xi^2 - 1)(1 - \eta^2)} \sin \varphi, \quad (6)$$

$$z = a\xi\eta. \quad (7)$$

Since H_0 has the rotational symmetry with respect to the molecular axis, the time-independent wave function can be written as

$$\psi_m(\xi, \eta, \varphi) = \Phi^m(\xi, \eta)e^{im\varphi}, \quad (8)$$

where m is the projection of the electron orbital angular momentum onto the molecular axis. m is a good quantum number if there is no laser field, or the laser field is along the molecular axis. We discretize ξ, η using a generalized pseudospectral method [34,35] and propagate the time-dependent wave function as

$$\Psi(t + \Delta t) = e^{-iH_0\Delta t/2} e^{-iV_{\text{ext}}(t)\Delta t} e^{-iH_0\Delta t/2} \Psi(t) \quad (9)$$

by the second-order split-operator method in the energy representation [36] with $\Psi(t = -\infty) = \Psi_g$, the ground-state wave function of H_2^+ . Once we obtain $\Psi(t)$, we can evaluate the time-dependent induced dipole moments as

$$d_z(t) = \langle \Psi(t) | z | \Psi(t) \rangle, \quad (10)$$

$$d_x(t) = \langle \Psi(t) | x | \Psi(t) \rangle, \quad (11)$$

where d_z (d_x) is the induced dipole moment parallel (perpendicular) to the molecular axis. Since the laser electric field is in the xz plane, the induced dipole moments are also in the xz plane. The power spectra of the HHG are obtained by the Fourier transformation of the induced dipole moments as

$$P_z(E) = \left| \frac{1}{\tau} \int_{-\infty}^{\infty} d_z(t) e^{-iEt} dt \right|^2, \quad (12)$$

$$P_x(E) = \left| \frac{1}{\tau} \int_{-\infty}^{\infty} d_x(t) e^{-iEt} dt \right|^2, \quad (13)$$

where E is the emitted photon energy. The total power spectra of the HHG can be written as a linear combination the two components, depending on the experimental setup. Using the molecular frame high-harmonic spectroscopy [30], one can single out the HHG yields corresponding to P_z or P_x .

III. RESULTS AND DISCUSSION

Using the above method, we investigate the HHG of H_2^+ in an intense laser field. Figure 1 shows the HHG power spectra of $P_z(E)$ when the laser polarization is along three different angles with respect to the molecular axis. The laser wavelength is 800 nm with a pulse duration of 15 fs and intensity of 10^{14} W/cm². For most of the HHGs, the yield decreases as the laser polarization angle θ increases. This tendency is consistent with Telnov's work [25], and it can be easily understood since the z component of the laser field strength decreases for increasing of the angle θ . The yield of the third-order harmonic drops by several orders of magnitude around $\theta = 30^\circ$ and increases again as θ increases further. By varying numerical simulation parameters—such as the number of grid points,

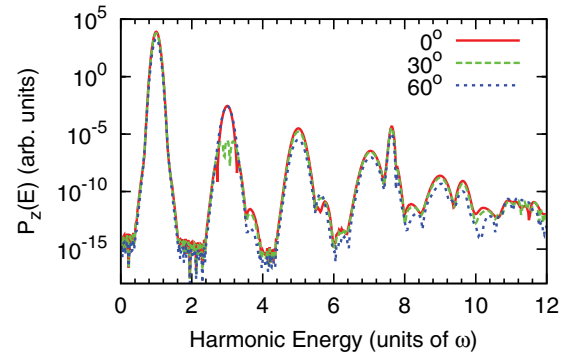


FIG. 1. (Color online) Power spectra $P_z(E)$ of the HHG for H_2^+ in an intense laser field when the laser polarization is along 0, 30, and 60 degrees. The H_2^+ is at the equilibrium distance $R = 2.0$ a.u. and the laser parameters: wavelength of 800 nm, pulse duration of 15 fs, and intensity of 10^{14} W/cm².

the box size, and absorber position—we confirmed that the minimum of the third-order harmonic at 30° is not accidental.

To explore the physical origin of the minimum, we plotted the yields of the third-order harmonic as a function of the angle between the molecular axis and the field polarization direction for three different wavelengths in Fig. 2. Although the angle of the minimum changes slightly as the laser wavelength changes, the minimum exists for all three cases. Thus we conclude that the minimum does not originate from resonant structures, since the processes involved in resonant structures are sensitive to the laser wavelength [32] or the nuclear separation [24].

For the induced dipole moment along the molecular axis, $d_z(t)$ can be further recast as a sum of each individual contributions of m state as $d_z(t) = \sum_m d_{z,m}(t)$, and the power spectra as well. We plotted $P_z(3\omega)$ and its major components from $m = 0$ (σ) and $m = 1$ (π) states in Fig. 3. We see that the yield of the third harmonic decreases at first as θ increases, reaches a minimum at 30° , and then increases again as θ increases. Finally, the yield drops again as θ approaches 90° , since the field component along the molecular axis is zero when the laser field is perpendicular to the molecular axis. In Fig. 3 we see that the σ states are the major contributor to the third-order harmonic when the laser field is almost along

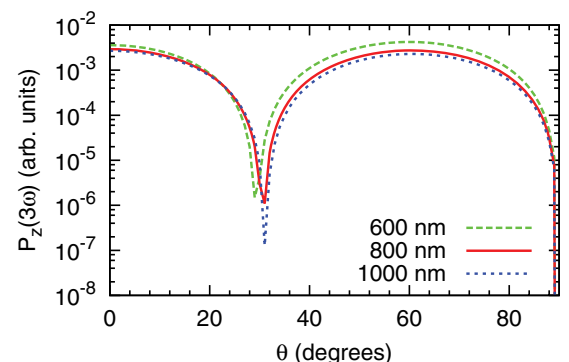


FIG. 2. (Color online) Yields of the third harmonic for the wavelengths of 600 nm (dashed line), 800 nm (solid line), and 1000 nm (dotted line). The other laser parameters are the same as in Fig. 1.

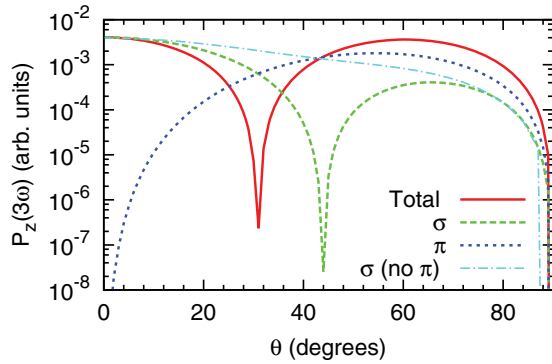


FIG. 3. (Color online) Yields of the third harmonic and the contributions from the σ (dashed curve) and π (dotted curve) states. The yield from σ states without π states in the time propagation is also plotted (dash-dotted curve). The laser parameters are the same as in Fig. 1.

the molecular axis. As the polarization angle increases, their contributions decrease while the contributions from π states increase. At 30° the two contributions from the σ and π states become equal. Since the power spectra of σ states are larger than the total power spectra when $\theta < 30^\circ$, the contribution of the π states must have an opposite sign from the one of the σ states. Cancellation of the two components results in the minimum of the power spectra at 30° . Interestingly, even the power spectra of P_z of the σ states only have a minimum around 45° , as shown in Fig. 3. If we remove the π states in the propagation of Eq. (1), the minimum disappears (dash-dotted curve in Fig. 3). The minimum at 45° comes from the indirect contribution of the π states in the time evolution of Eq. (1), in contrast with the minimum at 30° , which is caused by the direct cancellation of the dipole moments between the σ and π states. Since this minimum of the σ states at 45° is concealed by the π states in the total yield and cannot be observed in the experiment, we will not discuss its internuclear distance dependence and the laser intensity dependence.

Since the minimum of $P_z(3\omega)$ is not associated with the resonant structure, it should also exist for other internuclear distances. Figure 4 shows the yields of the third-order harmonic as a function of the internuclear distance R and laser polarization angle θ . We see a dark curved line representing the minima of the yields. The angle of the minimum increases

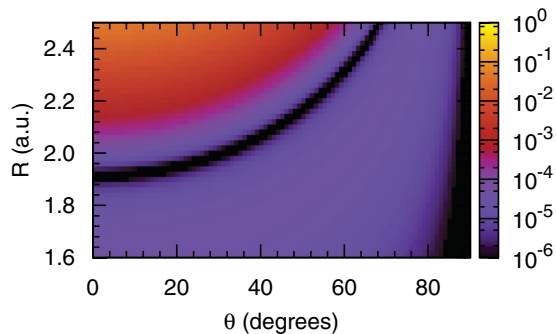


FIG. 4. (Color online) Power spectra $P_z(3\omega)$ of the third harmonic for H_2^+ as a function of the angle θ and the internuclear distance R . The laser parameters are the same as in Fig. 1.

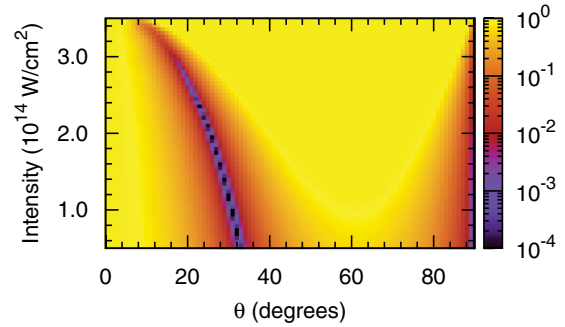


FIG. 5. (Color online) Power spectra of the third harmonic for H_2^+ as a function of the angle θ and the laser intensity. All the other laser parameters are the same as in Fig. 1.

as the internuclear distance increases. For small internuclear distance ($R < 1.8$ a.u.), there is no minimum. The minimum appears when the laser field is parallel to the molecular axis at $R \approx 1.9$. Then the minimum moves to a large angle when the internuclear distance R increases. When R increases further, in the separated-atom limit, the minimum disappears again. This infers that there is no minimum in atoms, either in the separated- or united-atom limit. This can be understood from the symmetry point of view since, for atoms, the HHG yield does not depend on the laser polarization direction.

In the following we investigate the laser intensity dependence of the minimum. Figure 5 shows the yield of the third-order harmonic as a function of the laser intensity and laser polarization angle θ . We see that the angle of the minimum decreases as the laser intensity increases, but the contrast becomes weaker. Comparing the relative yields from the σ and π states, we find that the yield from the π states becomes dominant as the angle θ increases for the high laser intensity. As we discussed above, the minimum appears when the contributions from the σ and π states are equal. If there is one dominant contributor, the minimum disappears. This confirms that the minimum is a general behavior for the third-order harmonic of H_2^+ in an intense laser field. The angle of the minimum depends on the laser intensity, internuclear distance, and so on. We may use those properties to extract the internuclear distance, laser information, and alignment parameters in the molecular frame high-harmonic spectroscopy.

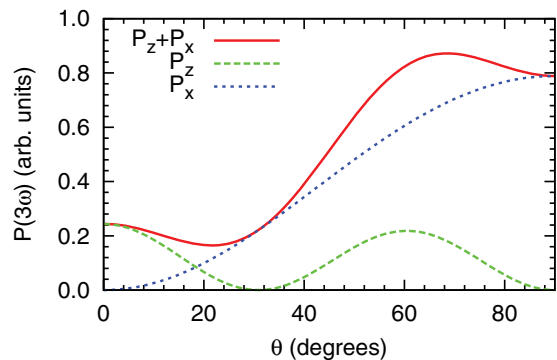


FIG. 6. (Color online) Power spectra of the third harmonic of H_2^+ and its components parallel (dashed curve) and perpendicular (dotted curve) to the molecular axis as a function of the angle θ . The laser parameters are the same as in Fig. 1.

So far, we only focused on the power spectra of the third-order harmonic for the dipole moment along the molecular axis. Figure 6 shows the total power spectra of the third-order harmonic and its components parallel and perpendicular to the molecular axis as a function of the laser polarization angle θ . We see that the angle of the minimum spreads over a large range in the linear scale. Different from P_z , the power spectrum of P_x increases monotonically as angle θ increases, its magnitude becomes larger than the one of P_z at $\theta = 20^\circ$. Conventionally the HHG comes mainly from the transitions from excited or continuum states to the ground state [37]. As shown in Fig. 3, the minimum appears when the transition to the excited states (π) is comparable to the transition to the ground state. This could be a general behavior when there are two radiative recombination pathways with comparable strengths.

To summarize, we have studied the HHG of H_2^+ ions in an intense laser field and found that there is a minimum for the third-order harmonic at a given laser polarization direction.

By decomposing the contributions from different molecular wave functions, we showed that the minimum is associated with the cancellation of the induced dipole moments from the σ and π states. Such a minimum may also exist for other molecular systems if the induced dipole moments originate from two equally important pathways. Since the position of the minimum depends on the molecular structures, laser parameters, one may extract the molecular bond length, the recombination time when the rescattering electron radiatively recombines with the parent-core, by measuring the third-order harmonic in the molecular frame [30].

ACKNOWLEDGMENTS

This research was supported by a Grand-in-Aid for Scientific Research from the Japan Society for the Promotion of Science and the HA-PACS Project for advanced interdisciplinary computational sciences by exa-scale computing technology.

-
- [1] X. F. Li, A. L'Huillier, M. Ferray, L. A. Lompre, and G. Mainfray, *Phys. Rev. A* **39**, 5751 (1989).
- [2] A. L'Huillier, K. J. Schafer, and K. C. Kulander, *J. Phys. B* **24**, 3315 (1991).
- [3] P. B. Corkum, *Phys. Rev. Lett.* **71**, 1994 (1993).
- [4] E. A. Gibson, A. Paul, N. Wagner, R. Tobey, S. Backus, I. P. Christov, M. M. Murnane, and H. C. Kapteyn, *Phys. Rev. Lett.* **92**, 033001 (2004).
- [5] J. J. Carrera, Shin-I Chu, and X. M. Tong, *Phys. Rev. A* **71**, 063813 (2005).
- [6] E. J. Takahashi, T. Kanai, K. L. Ishikawa, Y. Nabekawa, and K. Midorikawa, *Phys. Rev. Lett.* **101**, 253901 (2008).
- [7] E. J. Takahashi, P. Lan, O. D. Mücke, Y. Nabekawa, and K. Midorikawa, *Phys. Rev. Lett.* **104**, 233901 (2010).
- [8] Z. Chang, A. Rundquist, H. Wang, M. M. Murnane, and H. C. Kapteyn, *Phys. Rev. Lett.* **79**, 2967 (1997).
- [9] A. Rundquist, C. G. Durfee, Z. Chang, C. Herne, S. Backus, M. M. Murnane, and H. C. Kapteyn, *Science* **280**, 1412 (1998).
- [10] R. A. Bartels, A. Paul, H. Green, H. C. Kapteyn, M. M. Murnane, S. Backus, I. P. Christov, Y. Liu, D. Attwood, and C. Jacobsen, *Science* **297**, 376 (2002).
- [11] N. Milosevic, A. Scrinzi, and T. Brabec, *Phys. Rev. Lett.* **88**, 093905 (2002).
- [12] X. Wang, M. Chini, Q. Zhang, K. Zhao, Y. Wu, D. A. Telnov, Shin-I Chu, and Z. Chang, *Phys. Rev. A* **86**, 021802 (2012).
- [13] A. Willner, A. Hage, R. Riedel, I. Grguraš, A. Simoncig, M. Schulz, T. Dzelzainis, H. Höppner, S. Huber, M. J. Prandolini *et al.*, *Opt. Lett.* **37**, 3672 (2012).
- [14] M. Hentschel, R. Kienberger, C. Spielmann, G. A. Reider, N. Milosevic, T. Brabec, P. Corkum, U. Heinzmann, M. Drescher, and F. Krausz, *Nature (London)* **414**, 509 (2001).
- [15] G. Sansone, E. Benedetti, F. Calegari, C. Vozzi, L. Avaldi, R. Flammini, L. Poletto, P. Villoresi, C. Altucci, R. Velotta *et al.*, *Science* **314**, 443 (2006).
- [16] Y. Nomura, R. Hörlein, P. Tzallas, B. Dromey, S. Rykovanov, Z. Major, J. Osterhoff, S. Karsch, L. Veisz, M. Zepf *et al.*, *Nature Phys.* **5**, 124 (2009).
- [17] P. M. Paul, E. S. Toma, P. Breger, G. Mullot, F. Auge, P. Balcou, H. G. Muller, and P. Agostini, *Science* **292**, 1689 (2001).
- [18] E. Mansten, J. M. Dahlström, J. Mauritsson, T. Ruchon, A. L'Huillier, J. Tate, M. B. Gaarde, P. Eckle, A. Guandalini, M. Holler *et al.*, *Phys. Rev. Lett.* **102**, 083002 (2009).
- [19] E. Gagnon, P. Ranitovic, X. M. Tong, C. L. Cocke, M. M. Murnane, H. C. Kapteyn, and A. S. Sandhu, *Science* **317**, 1374 (2007).
- [20] A. S. Sandhu, E. Gagnon, R. Santra, V. Sharma, W. Li, P. Ho, P. Ranitovic, C. L. Cocke, M. M. Murnane, and H. C. Kapteyn, *Science* **322**, 1081 (2008).
- [21] P. Ranitovic, X. M. Tong, B. Gramkow, S. De, B. DePaola, K. P. Singh, W. Cao, M. Magrakvelidze, D. Ray, I. Bocharova *et al.*, *New J. Phys.* **12**, 013008 (2010).
- [22] P. Ranitovic, X. M. Tong, C. W. Hogle, X. Zhou, Y. Liu, N. Toshima, M. M. Murnane, and H. C. Kapteyn, *Phys. Rev. Lett.* **106**, 193008 (2011).
- [23] N. Shivaram, H. Timmers, X.-M. Tong, and A. Sandhu, *Phys. Rev. Lett.* **108**, 193002 (2012).
- [24] D. A. Telnov and Shin-I Chu, *Phys. Rev. A* **71**, 013408 (2005).
- [25] D. A. Telnov and Shin-I Chu, *Phys. Rev. A* **76**, 043412 (2007).
- [26] J. Itatani, J. Levesque, D. Zeidler, H. Niikura, H. Pepin, J. C. Kieffer, P. B. Corkum, and D. M. Villeneuve, *Nature (London)* **432**, 867 (2004).
- [27] A.-T. Le, R. R. Lucchese, M. T. Lee, and C. D. Lin, *Phys. Rev. Lett.* **102**, 203001 (2009).
- [28] C. D. Lin, A.-T. Le, Z. Chen, T. Morishita, and R. Lucchese, *J. Phys. B* **43**, 122001 (2010).
- [29] J. W. Cooper, *Phys. Rev.* **128**, 681 (1962).
- [30] J. B. Bertrand, H. J. Wörner, P. Hockett, D. M. Villeneuve, and P. B. Corkum, *Phys. Rev. Lett.* **109**, 143001 (2012).
- [31] I. Ben-Itzhak, P. Q. Wang, A. M. Sayler, K. D. Carnes, M. Leonard, B. D. Esry, A. S. Alnaser, B. Ulrich,

- X. M. Tong, I. V. Litvinyuk *et al.*, *Phys. Rev. A* **78**, 063419 (2008).
- [32] Y.-J. Jin, X.-M. Tong, and N. Toshima, *Phys. Rev. A* **81**, 013408 (2010).
- [33] Y.-J. Jin, X.-M. Tong, and N. Toshima, *Phys. Rev. A* **83**, 063409 (2011).
- [34] D. A. Telnov and Shin-I Chu, *Phys. Rev. A* **59**, 2864 (1999).
- [35] X. Chu, *Phys. Rev. A* **82**, 023407 (2010).
- [36] X. M. Tong and Shin-I Chu, *Chem. Phys.* **217**, 119 (1997).
- [37] M. Lewenstein, P. Balcou, M. Y. Ivanov, A. L'Huillier, and P. B. Corkum, *Phys. Rev. A* **49**, 2117 (1994).